Journal of Chromatography A, 1218 (2011) 5273–5278

Contents lists available at ScienceDirect

Journal of Chromatography A

journal homepage: www.elsevier.com/locate/chroma

Monolith-based immobilized metal affinity chromatography increases production efficiency for plasmid DNA purification

Min Jae Shin[a], Lihan Tan[b], Min Ho Jeong[a], Ji-Heung Kim[a], Woo-Seok Choe[a,*]

[a] School of Chemical Engineering, Sungkyunkwan University, Suwon 440-746, South Korea
[b] Department of Chemical and Biomolecular Engineering, National University of Singapore, 10 Kent Ridge Crescent 117576, Singapore

ARTICLE INFO

Article history:
Received 18 February 2011
Received in revised form 3 June 2011
Accepted 8 June 2011
Available online 17 June 2011

Keywords:
Immobilized metal affinity chromatography (IMAC)
Monolith column
Particle-based column
Plasmid DNA purification
RNA dynamic binding capacity

ABSTRACT

Immobilized metal affinity monolith column as a new class of chromatographic support is shown to be superior to conventional particle-based column as plasmid DNA (pDNA) purification platform. By harnessing the affinity of endotoxin to copper ions in the solution, a majority of endotoxin (90%) was removed from the alkaline cell lysate using $CuCl_2$-induced precipitation. RNA and remaining endotoxin were subsequently removed to below detection limit with minimal loss of pDNA using either monolith or particle-based column. Monolith column has the additional advantage of feed concentration and flowrate-independent dynamic binding capacity for RNA molecules, enabling purification process to be conducted at high feed RNA concentration and flowrate. The use of monolith column gives three fold increased productivity of pDNA as compared to particle-based column, providing a more rapid and economical platform for pDNA purification.

1. Introduction

Plasmid DNA (pDNA) vaccine consists of circular and double stranded extra chromosomal DNA encoding specific gene of one or more protein antigens [1]. In the host cells, the production of protein antigens induces humoral (antibody) and cellular (T cell) immune responses [2]. Plasmid DNA vaccines, compared to the conventional vaccines, have potential advantages such as eliminating the risk of viral infections via vaccination process and life-long immunity against several diseases in a single dose [3]. The quality of pDNA for therapeutics has to meet regulatory specifications in terms of purity, homogeneity and potency (>95% supercoiled (sc) pDNA, undetectable RNA on agarose gel electrophoresis and <0.1 EU/μg plasmid by LAL assay for endotoxin) [4].

pDNA purification using affinity precipitation (with compacting agents such as spermine [5] and spermidine [5,6] or high salt concentration such as 2.5 M ammonium sulfate [7]) and various chromatography procedures (e.g. size, charge, hydrophobicity, affinity-related chromatography) [8] have been reported. The scaling up to an industrial process scale for conventional particle-based column chromatography, however, has some disadvantages including high pressure drop, low flowrate and channeling flow [9]. Besides for macromolecules such as pDNA and RNA, the access to intraparticle pores of particle-based column is restricted by the large size of macromolecules, hence resulting in low binding capacity and throughput as the interaction between the target molecules and immobilized metal ions occurs mainly on the external particle surface of the chromatographic support [10].

Recently, monolith-based chromatography suitable for separation and purification of macromolecules is developed [11–13]. In a monolith column, due to high porosity, the pressure drop is low and stationary phase structure is intact even at a high flowrate [14]. Moreover, the separation and purification process based on convective flow can result in flow-independent resolution and dynamic binding capacity even for macromolecules [15,16]. Using $CaCl_2$ precipitation and a combination of monolith-based anion exchange and hydrophobic interaction chromatographic procedures, separation of scpDNA from impurities such as open circular (oc) pDNA, genomic DNA (gDNA), RNA and endotoxin was achieved [12]. The purification of pDNA harboring *lacO* nucleotide sequences from pDNA lacking *lacO* was also enabled in a single unit operation using LacI based peptide-monolith construct [13].

In our previous study, $CuCl_2$-induced precipitation followed by Cu^{2+}-iminodiacetic acid (IDA) based immobilized metal affinity chromatography (IMAC) were conducted to purify pDNA from its contaminants in the batch binding mode [17]. In brief, pDNA, RNA and endotoxin were precipitated by free Cu^{2+} ions from alkaline cell lysate while the majority of other impurities remain in the supernatant. After pDNA and RNA were transferred into bulk solution by adding EDTA to the precipitates, RNA could be selectively

* Corresponding author. Tel.: +82 31 290 7344; fax: +82 31 290 7272.
E-mail address: checws@skku.edu (W.-S. Choe).

0021-9673/$ – see front matter © 2011 Elsevier B.V. All rights reserved.
doi:10.1016/j.chroma.2011.06.040

captured by Cu^{2+} ions immobilized on the IDA particles, enriching pDNA in the unbound fraction. It was shown that RNA and endotoxin were completely removed from alkaline cell lysate without significant loss of pDNA. The interaction of nucleic acids with immobilized Cu^{2+} ions is based on affinity between exposed aromatic nitrogen bases in the nucleic acids and the metal ions [18]. Hence, pDNA where aromatic nitrogen bases were hidden within the double stranded helical structure did not show affinity to the immobilized metal ions while single stranded RNA with exposed aromatic nitrogen bases exhibited interaction with the metal ions.

However, the purification of pDNA in the chromatographic mode would be indispensable for efficient large scale operation. Since RNA is the major contaminant in the alkaline cell lysate following the $CuCl_2$-induced clearance of the majority of endotoxin, this study first investigated the dynamic binding capacity of RNA molecules to metal affinity monolith or particle-based column using feedstock solutions with or without the co-presence of pDNA at different feed concentrations and flowrates and assessed the RNA removal efficiencies and pDNA productivities in pDNA purification process at various chromatographic separation conditions.

2. Experimental

2.1. Materials

The particle-based and monolith IMAC columns used were HiTrap Chelating HP column (GE Healthcare, 17-0408-01) and CIM IDA disk monolithic column (BIA separation, 217.3010), respectively. Reagents used were tris (Applichem, A2264.1000), sodium chloride (Duksan, SEE0-32201), agarose (Promega, DV3125), ethidium bromide solution (Fluka, 46067), 1 kb plus 100 bpDNA ladder (Mbiotech, 10103), low MW DNA ladder (New England Biolabs, N3233S) and gel loading dye blue 6× (Biolabs, B7021). Baker's yeast RNA (R6750), endotoxin removal solution (E4274), cupric chloride dihydrate (C3279), imidazole (I2399) and EDTA disodium dihydrate (E5134) were from Sigma. SnakeSkin Dialysis Tubing with a nominal MWCO of 3.5 kDa (68035) was supplied by Perbio Science, and Endofree DNA Maxi purification kit (12362) by Qiagen.

2.2. Fermentation and alkaline cell lysis

DH5-α mutant harboring plasmid pcDNA3.1D, a 7.3 kb high copy plasmid (100–200/cell) which contains 1.8 kb dengue fever antigenic gene (NS3), was kindly provided by Bioprocessing Technology Institute (Singapore). Cells were grown on 12 g/l yeast extract (Conda Pronadisa, 1702.00), 6 g/l tryptone (Conda Pronadisa, 1612.00), 5 g/l glucose (Sigma, G8270), 6 g/l K_2HPO_4 (Aldrich, 221317) and 0.48 g/l $MgSO_4$ (Sigma–Aldrich, M7506) using 250 ml shake flasks in a shaking incubator (50 ml culture volume, 16 h, 37 °C, 250 rpm). Cell lysate was obtained using alkaline cell lysis procedures as described previously [19].

2.3. $CuCl_2$-induced precipitation prior Cu^{2+}-IDA based IMAC

To 30 ml of alkaline cell lysate, powdered $CuCl_2$ was added to a final concentration of 0.75 M, incubated on the mixer at 30 rpm for 15 min and centrifuged (19,000 × *g* for 1 min). After washing the precipitate with 30 ml (2 × 15 ml) of Tris buffer (20 mM Tris, pH 7), 30 ml of 50 mM EDTA in Tris buffer was added to the precipitate. 20 ml of the resulting supernatant was dialyzed against Tris–NaCl buffer (20 mM Tris, 0.75 M NaCl, pH 7) using SnakeSkin Dialysis Tubing (12–16 h) and concentrated using Amicon Ultra-15 Centrifugal Filter Units with a nominal MWCO of 3 kDa (Millipore, UFC900324). The dialyzed solution was filtered with 0.2 μm Minisart NML from Sartorius (16534-K) prior to CIM IDA disk monolith or HiTrap Chelating HP column loading.

2.4. Dynamic binding capacities for RNA molecules in various feedstock solutions using monolith and particle-based columns

Both CIM IDA disk monolithic column (comprising 3 disks of 0.34 ml volume per disk) and HiTrap Chelating HP column (1 ml) were washed with water (2 × 5 column volume (CV)), charged with 100 mM $CuCl_2$ (5 CV), washed with water (2 × 5 CV), and equilibrated with Tris–NaCl buffer (2 × 10 CV). Baker's yeast RNA was stripped of endotoxin using endotoxin removal solution. The purified RNA devoid of endotoxin (<0.05 EU/ml) was dissolved in Tris–NaCl buffer to give RNA concentrations in the range of 0.05, 0.1, 0.5, 1.0 and 2.0 mg/ml. RNA solutions were processed at flowrate of 0.5, 1, 2, 3, 6 and 9 ml/min for CIM IDA disk monolith column, and 0.5, 1, 2 and 3 ml/min for HiTrap Chelating HP column using a FPLC system (Bio-Rad, 760-2266) equipped with UV detector at 260 nm for continuous monitoring of RNA content in the flow-through.

The above procedures were repeated for cocktail solution (containing pDNA from Endofree DNA purification kit (<0.05 EU/ml) and purified RNA) and partially purified alkaline cell lysate with 222 EU/mL endotoxin (using $CuCl_2$-induced precipitation followed by EDTA resolubilization and dialysis against Tris–NaCl buffer) at 1 ml/min feed flowrate. In both cases, pDNA at concentrations of 0.016 and 0.002 mg/ml co-existed with RNA at concentrations of 1.0 and 0.1 mg/ml, respectively.

RNA molecules bound to the columns for various feedstock solutions were eluted using 500 mM imidazole. The amount of eluted RNA was quantified by agarose gel densitometry method as described in Section 2.5.1, and termed as dynamic binding capacity of RNA.

All experiments were performed in duplicates and the results averaged.

2.5. Analytical methods

2.5.1. Plasmid DNA (pDNA) and RNA analysis

Standard pure pDNA or RNA was quantified at 260 nm by UV/Vis spectrophotometer (WPA Biowave-2, Biochrom, 80-3003-75). 1 or 2% agarose gel electrophoresis was conducted in TAE buffer (40 mM Tris–acetate, 1 mM EDTA, pH 8) using Mupid 2-plus (Advance, AD110) at 100 V for 25 min. Denatured loading samples were prepared prior to mixing with 6× loading dye as follows: 20 μl analyte, 150 μl formamide (Junsei, 377F0440, 98.5, v/v%)and 30 μl water were mixed, heated for 5 min at 95 °C, and immediately chilled on ice for 5 min in order to eliminate the effects of secondary RNA structure and base pairing on RNA electrophoretic mobility. The gel (containing 0.01% ethidium bromide) was then imaged by GelDoc-It Imaging System (UVP, 97-0139-04) and pDNA or RNA quantified with purified pDNA or Baker's yeast RNA as standard, respectively, using VisionWorksLS software equipped with the imaging system.

2.5.2. Endotoxin analysis

Endotoxin detection reagents used were Pyrochrome Chromogenic Endotoxin Testing (C1500), Control Standard Endotoxin (EC010) and LAL Reagent Water (WP1001) from Cape Cod Incorporated. The samples for endotoxin analysis were prepared in sterile polystyrene culture tubes (BD Falcon, 352052). Each sample was mixed with pyrochrome reagent and incubated at 37 °C for 30 min prior to UV absorbance reading at 405 nm using a microplate reader (Molecular Devices, EMax). Endotoxin concentration was calculated from endotoxin standard curve using SoftMax Program 4.6 according to manufacturer's instructions.

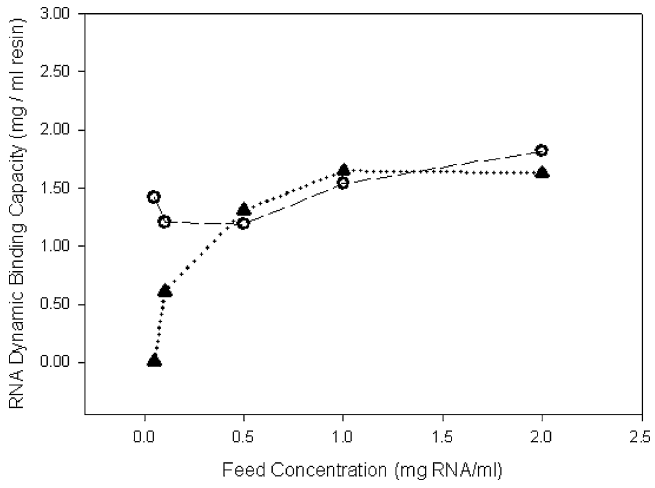

Fig. 1. RNA dynamic binding capacities at various feed concentrations for monolith (○) and particle-based (▲) columns at 1 ml/min feed flowrate.

3. Results and discussion

Following $CuCl_2$-induced precipitation, 90% of endotoxin (from 2246 to 222 EU) was removed from alkaline cell lysate (Table 1). As RNA was the major remaining contaminant in the resulting processing liquor, RNA binding characteristics to monolith or particle-based Cu^{2+}-charged metal affinity column under different feed concentrations and flowrates were studied to identify the optimal condition for pDNA purification.

3.1. Dynamic binding capacity of RNA

3.1.1. Effect of feed concentration on dynamic binding capacity profiles of RNA

In order to investigate the dynamic binding capacity of RNA molecules to Cu^{2+}-charged IDA monolith and conventional particle-based columns at various feed concentrations (0.05–2.0 mg/ml), purified baker's yeast RNA designated as Solution I was used.

The dynamic binding capacity profiles of RNA obtained with the Solution I for both monolith and particle-based columns are shown in Fig. 1. As feed RNA concentration is increased for particle-based column, higher dynamic binding capacity of RNA molecules is shown prior to reaching a plateau of 1.65 mg RNA/ml resin at feed concentration of 1.0 mg RNA/ml feed, while the dynamic binding capacity (average 1.20 mg RNA/ml resin) is independent of RNA feed concentration for monolith column.

The different trend in RNA dynamic binding capacities for particle-based and monolith-based columns could be due to two factors: the different characteristics of chromatographic supports (e.g. pore and/or channel size) between both columns, and the excluded-volume effect of RNA molecules. Most of the conventional particle-based chromatographic supports are typically constructed from particles with intraparticle pore diameter of 30–400 nm, and hence macromolecules such as RNA with a size of 100 nm to over 300 nm in diameter could not effectively make use of the binding sites available in the pore region [20]. As the concentration of RNA in feedstock solution increases, however, RNA molecules tend to form more compact structure in order to reduce negative charge repulsion between neighboring RNA molecules (i.e. excluded-volume effect) [21]. Hence, as RNA concentration in the feedstock increases, the compacted RNA molecules facilitate the access to pore-ligand as well as surface-ligand, giving rise to the dynamic binding capacity increase for particle-based column.

Table 1
The comparison of the pDNA purification productivity (ζ) from alkaline cell lysate using either monolith or particle-based column.

Process	Chromatographic support	pDNA		RNA		Endotoxin		EU/μg pDNA	Flowrate (ml/min)	RNA removal efficiency (ε) (mg RNA/ml/h)	Productivity (ζ) (mg pDNA/ml/h)
		mg	Recovery (%)	mg	Removal (%)	EU	Removal (%)				
Alkaline cell lysis	–	0.010	–	1.46	–	2246	–	–	–	–	–
$CuCl_2$-precipitation, EDTA resolubilization and dialysis	–	0.010	~100	1.46	0	222	90	–	–	–	–
Cu^{2+}-IDA IMAC	Monolith	0.010	~100	0	~100	<0.05	~100	<0.005	9	1.577	10.80
	Particle-based	0.009	90	0	~100	<0.05	~100	<0.005	3	0.527	3.24

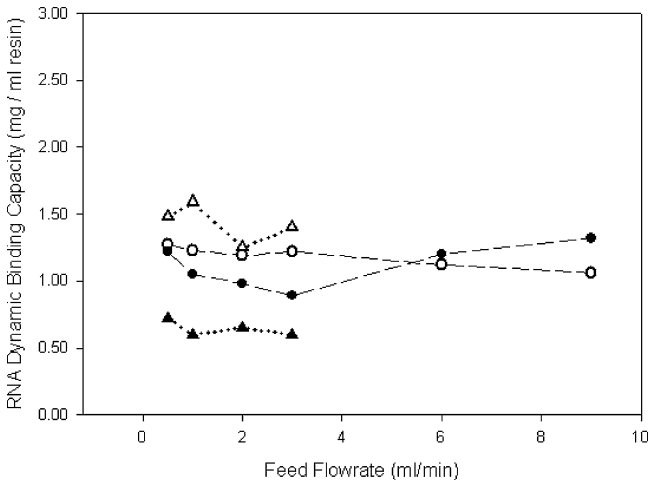

Fig. 2. RNA dynamic binding capacities at various feed flowrates for monolith (●, ○) and particle-based (▲, △) columns at 0.1 and 1.0 mg RNA/ml feed, respectively.

On the contrary, monolith-based chromatographic supports with large channel size of 700–1000 nm allow full utilization of the ligands on the chromatographic resin even at low feed concentration (with incompact structure of RNA), resulting in concentration-independent dynamic binding capacity for RNA molecules [14,22]. Thus the enhanced process efficiency with the use of monolith column is especially highlighted at low RNA feed concentration.

3.1.2. *Effect of feed flowrate on dynamic binding capacity profiles of RNA*

The effect of feed flowrate, one of the critical factors which could affect the dynamic binding capacity of RNA molecules to Cu^{2+}-charged IDA for monolith and conventional particle-based columns, was investigated with the use of Solution I.

Fig. 2 shows the dynamic binding capacity for RNA at different feed flowrates from 0.5 to 9 ml/min for monolith column and 0.5–3 ml/min for particle-based column (which are up to recommended maximum flowrate by each provider). For the conventional particle-based column, it could be processed only at low feed flowrates due to bed compression at higher flowrates [23,24]. The dynamic binding capacities of RNA molecules are determined as follows: average 1.11 and 1.18 mg RNA/ml resin at 0.1 and 1.0 mg RNA/ml, respectively for monolith column, and average 0.64 and 1.43 mg RNA/ml resin at 0.1 and 1.0 mg RNA/ml, respectively for particle-based column in the flowrate range investigated. The dynamic binding capacities of RNA molecules are independent of feed flowrates when the feed RNA concentration is fixed for particle-based column. For monolith column, the dynamic binding capacities of RNA molecules are found to be flowrate-independent regardless of feed concentrations. The effect of flowrate on dynamic binding capacity of RNA molecules on either monolith or particle-based column matrix is rarely found in the literature. For adsorption of scpDNA to particle-based chromatographic supports (e.g. histidine-agarose chromatography [25]), the dynamic binding capacity of pDNA molecules was found to decrease at higher feed flowrates. This is presumably due to a combination of the extension of pDNA molecules (by high flowrate driven external hydrodynamic forces) [21] and shorter time allowed for pDNA to ligand interaction at high flowrate which enabled fewer molecules to access the ligands on the resin (especially for the ligands in the intraparticle pores) [25]. On the other hand, adsorption of pDNA to anion-exchange DEAE (diethylaminoethyl) monolith column was reported to be flowrate-independent from 120 to 335 cm/h for 39.4 kbp pDNA [26] and from

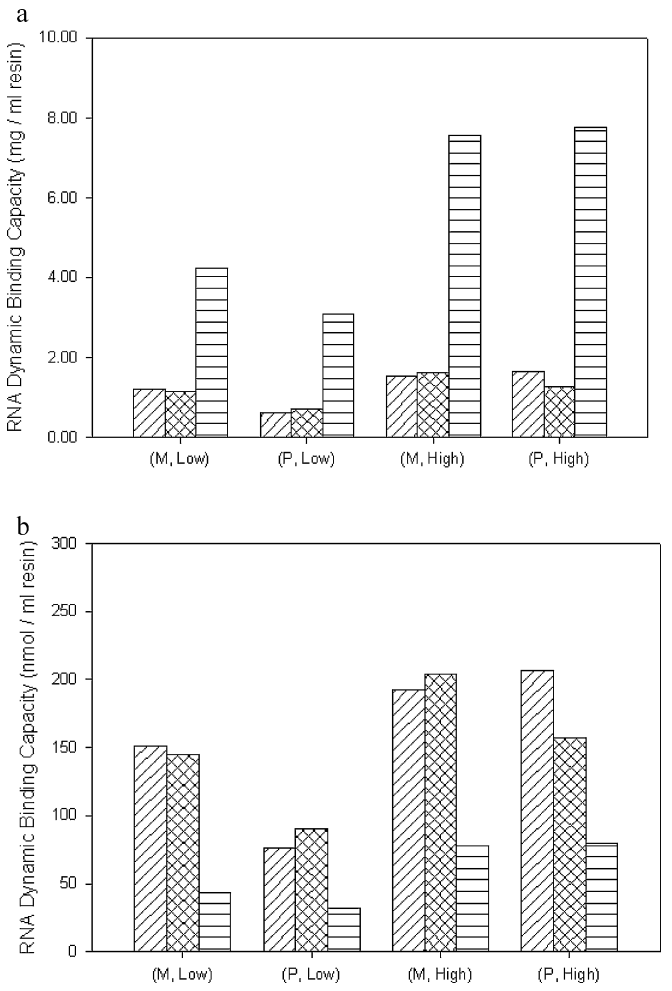

Fig. 3. RNA dynamic binding capacities (in terms of (a) mg/ml resin or (b) nmol/ml resin) for monolith (M) or particle-based (P) columns at 0.1 (low) and 1.0 (high) mg RNA/ml feed in various feedstock environments: pure RNA solution (Solution I) (▨), cocktail solution (Solution II) (▩) and partially purified alkaline cell lysate (Solution III) (▭).

500 to 1000 cm/h for 6.9 kbp pDNA [20]. The lack of flowrate dependence could be explained by the large channel size for monolith column which does not hinder pDNA to ligand interaction despite the extension of pDNA at higher flowrates. However, for single-stranded RNA, the extension of molecules at higher flowrates is likely to be minimal due to the linear structure of RNA molecules as compared to supercoiled pDNA molecules. This together with the smaller molecular weight of RNA (and hence less affected by the decrease in interaction time between RNA and the binding ligand as RNA can access the intraparticle pores with greater ease) gives rise to flowrate-independent RNA dynamic binding capacity regardless of types of chromatographic support.

3.2. *Verification of RNA dynamic binding capacity in the co-presence of plasmid DNA*

To further investigate the influence of other molecules such as pDNA and endotoxin on RNA dynamic binding capacity, three different feedstock solutions were prepared as follows: (1) purified baker's yeast RNA lacking endotoxin (Solution I); (2) cocktail solution comprising purified pDNA and RNA (Solution II); (3) partially purified alkaline cell lysate mostly comprising pDNA and RNA following 90% removal of endotoxin via $CuCl_2$-induced precipitation, EDTA resolubilization and dialysis (Solution III). Fig. 3 shows the

Table 2
RNA removal efficiencies (ε, mg RNA/ml resin/h) from pure RNA solution using either monolith or particle-based column.

Chromatographic support	Feed concentration (mg/ml)	Feed flowrate (ml/min)					
		0.5	1	2	3	6	9
Monolith column	0.05	–	0.085	–	–	–	–
	0.1	0.037	0.068	0.118	0.160	0.432	0.713
	0.5	–	0.071	–	–	–	–
	1.0	0.038	0.083	0.143	0.220	0.403	0.572
	2.0	–	0.109	–	–	–	–
Particle-based column	0.05	–	0.001	–	–	–	–
	0.1	0.022	0.036	0.078	0.108	–	–
	0.5	–	0.079	–	–	–	–
	1.0	0.044	0.097	0.150	0.252	–	–
	2.0	–	0.098	–	–	–	–

RNA dynamic binding capacities for monolith and particle-based columns when these three RNA solutions with or without pDNA and small amount of endotoxin were applied to the columns at two different RNA feed concentrations (0.1 and 1 mg/ml) and a fixed flowrate of 1 ml/min. In Solution II, it was found that RNA binding to either monolith or particle-based Cu^{2+}-IDA was unaffected by the presence of pDNA as shown in Fig. 3a. In Solution III, however, the apparent RNA dynamic binding capacities in terms of mg RNA/ml resin significantly increased for both monolith and particle-based columns compared with those of RNA molecules in pure RNA (Solution I) and cocktail solutions (Solution II). RNA molecules (average 300 nucleotides, 0.097 mg/nmol) in partially purified alkaline cell lysate (Solution III) have twelve-fold larger molecular weight than the Baker's yeast RNA molecules (average 25 nucleotides, 0.008 mg/nmol) used for preparation of Solutions I and II (Fig. 4). Considering the significant difference in the molecular weight of two types of RNA, the apparent RNA dynamic binding capacities exhibited for monolith and particle-based columns were recalculated in terms of molar dynamic binding capacities (i.e. nmol RNA/ml resin) as shown in Fig. 3b. In comparison of Fig. 3a and b, it was found that molar RNA dynamic binding capacities for monolith and particle-based columns decreased significantly when RNA existed together with pDNA and endotoxin as in the case of Solution III. Since pDNA was found not to interfere with the binding of RNA to Cu^{2+}-IDA on both column matrices, this can be explained in two aspects: (1) high molecular weight RNA molecules residing in Solution III are likely to occupy more of the Cu^{2+}ligands per RNA molecule and hence result in less number of RNA molecules captured per unit resin volume; (2) the presence of endotoxin (i.e. approximately 10% of entrained endotoxin after partial purification of the initial alkaline cell lysate) is envisaged to compromise the metal ion binding sites available for RNA as endotoxin was shown to have a higher affinity than RNA [19]. Taken together, the RNA dynamic binding capacities are unaffected by the co-presence of pDNA (i.e. Solution I vs. Solution II) but are dependent on the RNA molecular weight and the presence of endotoxin (i.e. Solution II vs. Solution III) for both monolith and particle-based columns.

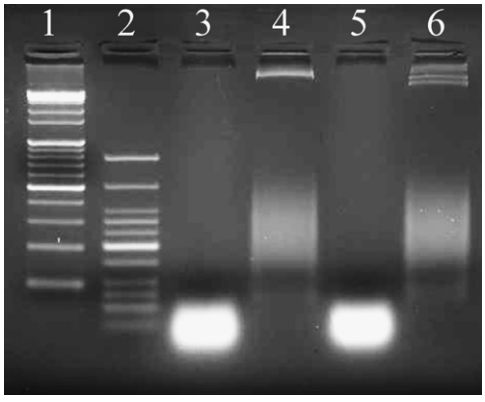

Fig. 4. The comparison of RNA molecular weight in various feedstock solutions analyzed on 2% agarose gel electrophoresis. Lanes: 1, DNA marker (Mbiotech, 10103); 2, DNA marker (New England Biolabs, N3233S), 3, pure RNA solution (Solution I, native form); 4, partially purified alkaline cell lysate (Solution III, native form); 5, pure RNA solution (Solution I, denatured by hot formamide); 6, partially purified alkaline cell lysate (Solution III, denatured by hot formamide).

3.3. Overall efficiency comparison of monolith with particle-based column procedure

The overall process efficiency for monolith and particle-based columns was determined by RNA removal efficiency (ε) defined as the amount of RNA removed from feedstock per unit resin volume per unit process time (i.e. $M_{RNA}/V_{resin}/t_{process}$, mg RNA/ml resin/h) with the use of 1000 ml feedstock as a basis for calculation. Taking α mg/ml RNA in the feedstock as feed concentration, β ml/min as feed flowrate, γ mg/ml resin as dynamic binding capacity and δ ml as total process volume for monolith and particle-based columns, M_{RNA}, V_{resin}, $t_{process}$ and ε were computed as $\delta^*\alpha$, $\delta^*\alpha/\gamma$, $\delta/\beta/60$ and $(60^*\beta^*\gamma)/\delta$, respectively.

Table 2 shows the RNA removal efficiencies (ε) for monolith and particle-based columns calculated at various feed concentrations and flowrates. For particle-based column, as RNA feed concentration increases from 0.05 to 2.0 mg/ml and as flowrate increases from 0.5 to 3 ml/min, ε increases proportionally. The highest value for ε (0.252 mg RNA/ml resin/h) is obtained at RNA feed concentrations above 1.0 mg/ml and a feed flowrate of 3 ml/min. This is attributed to the constant dynamic binding capacity (i.e. 1.65 mg RNA/ml resin) above RNA concentration of 1.0 mg/ml in the feedstock (Fig. 1) and the reduction of process time with the increase in the feed flowrate. For monolith column, the efficiency of RNA removal is dependent mostly on feed flowrate and relatively independent of feed concentration. The high values for ε at 0.713 mg RNA/ml resin/h and 0.572 mg RNA/ml resin/h are obtained at feed flowrate of 9 ml/min for RNA feed concentration of 0.1 and 1.0 mg RNA/ml, respectively. Thus monolith column shows 2.3–6.6 fold higher value for ε over particle-based column in the range of feed RNA concentrations and flowrates investigated.

Finally, in order to assess the productivity of pDNA purification processes employing either monolith or particle-based column, alkaline cell lysate containing 0.010 mg pDNA, 1.46 mg RNA and 2246 EU endotoxin was prepared. Following the removal of 90% of endotoxin by $CuCl_2$-precipitation, EDTA resolubilization and dialysis, the partially purified alkaline cell lysate containing 0.010 or

0.009 mg pDNA, 1.46 mg RNA and 222 EU endotoxin was obtained and used as a feedstock for the column procedure using either monolith or particle-based resin. The overall purification process performance is summarized in Table 1. Both monolith and particle-based column procedures shows high recoveries of pDNA (at least >90%) with successful removal of RNA and endotoxin below the detection limit specified. The productivities of pDNA purification defined as the amount of pDNA purified from feedstock per unit resin volume per unit process time (i.e. $M_{pDNA}/V_{resin}/t_{process}$, mg pDNA/ml resin/h) were calculated to be 10.80 and 3.24 mg pDNA/ml resin/h for monolith and particle-based column procedures, respectively, making the use of monolith column beneficial and ideal for large-scale pDNA purification process. The volumetric flowrates of 0.5–3 ml/min for particle-based column in the present study correspond to 80–470 cm/h in terms of the linear velocities, in a good agreement with those typically employed for conventional particle-based columns (i.e. 100–300 cm/h) [20]. However, the investigated volumetric flowrate range for monolith column (i.e. 0.5–9 ml/min) is equivalent to the linear velocity range (30–480 cm/h), much lower than that (500–1000 cm/h) reported at industrial scale [20]. Therefore, for the large scale use of monolith column where the feed flowrate could be further increased, the process efficiency of pDNA purification might be further enhanced.

4. Conclusions

This study proves that monolith-based chromatographic support, which possesses lower mass transfer limitation and higher throughput than the conventional particle-based supports, is advantageous for purification of pDNA in terms of approximately three fold higher pDNA productivity (ζ) and RNA removal efficiency (ε). Further processing steps may be required to separate genomic DNA (gDNA) and/or pDNA isoforms prior to obtaining scpDNA of therapeutic grade. However, a combination of $CuCl_2$-induced precipitation, EDTA resolubilization, dialysis and monolith-based Cu^{2+}-IDA IMAC exhibits concentration-independent efficient removal of RNA and endotoxin along with complete recovery of pDNA at high flowrate, and therefore provides an economically viable new platform for pDNA purification.

Acknowledgments

This work was financially supported by the Ministry of Education, Science and Technology (MEST) and the Ministry of Knowledge Economy (MKE) to foster the development of the Industrial-Academic Cooperation Centered University.

References

[1] H.S. Garmory, Genet. Vaccines Ther. 1 (2003).
[2] M. Schleef, Plasmids for Therapy and Vaccination, Wiley-VCH, 2001.
[3] H.L. Robinson, Am. Acad. Microbiol. (1997).
[4] G.N.M. Ferreira, G.A. Monteiro, D.M.F. Prazeres, J.M.S. Cabral, Trends Biotechnol. 18 (2000) 380.
[5] D.V. Mourich, M.W. Munks, J.C. Murphy, R.C. Willson, A.B. Hill, J. Immunol. Methods 274 (2003) 257.
[6] J.C. Murphy, J.A. Wibbenmeyer, G.E. Fox, R.C. Willson, Nat. Biotechnol. 17 (1999) 822.
[7] M.M. Diogo, J.A. Queiroz, G.A. Monteiro, S.A.M. Martins, G.N.M. Ferreira, D.M.F. Prazeres, Biotechnol. Bioeng. 68 (2000) 576.
[8] M.M. Diogo, J.A. Queiroz, D.M.F. Prazeres, J. Chromatogr. A 1069 (2005) 3.
[9] R. Ghosh, J. Chromatogr. A 952 (2002) 13.
[10] D.M.F. Prazeres, T. Schluep, C. Cooney, J. Chromatogr. A 806 (1998) 31.
[11] F. Svec, J. Chromatogr. Libr. (2003).
[12] F. Smrekar, A. Podgornik, M. Ciringer, S. Kontrec, P. Raspor, A. Strancar, M. Peterka, Vaccine 28 (2010) 2039.
[13] Y. Han, G. You, L.K. Pattenden, G.M. Forde, Process Biochem. 45 (2010) 203.
[14] I. Mihelic, T. Koloini, A. Podgornik, A. Strancar, HRC-J. High Resolut. Chromatogr. 23 (2000) 39.
[15] G. Iberer, R. Hahn, A. Jungbauer, Monoliths As Stationary Phases for Separation of Biopolymers: The Fourth Generation of Chromatography Sorbents, LC–GC, Europe, 1999.
[16] A. Podgornik, M. Barut, A. Strancar, D. Josic, T. Koloini, Anal. Chem. 72 (2000) 5693.
[17] L.H. Tan, D.S. Kim, I.K. Yoo, W.S. Choe, Chem. Eng. Sci. 62 (2007) 5809.
[18] J.C. Murphy, D.L. Jewell, K.I. White, G.E. Fox, R.C. Willson, Biotechnol. Prog. 19 (2003) 982.
[19] L.H. Tan, W.B. Lai, C.T. Lee, D.S. Kim, W.S. Choe, J. Chromatogr. A 1141 (2007) 226.
[20] J. Urthalera, R. Schlegl, A. Podgornik, A. Strancar, A. Jungbauer, R. Necina, J. Chromatogr. A 1065 (2005) 93.
[21] C. Haber, J. Skupsky, A. Lee, R. Lander, Biotechnol. Bioeng. 88 (2004) 26.
[22] A. Strancar, A. Podgornik, M. Barut, R. Necina, Adv. Biochem. Eng./Biotechnol. (2002) 49.
[23] M.W.H. Roberts, C.M. Ongkudon, G.M. Forde, M.K. Danquah, J. Sep. Sci. 32 (2009) 2485.
[24] K.F. Du, D. Yang, Y. Sun, J. Chromatogr. A 1163 (2007) 212.
[25] F. Sousa, D.M.F. Prazeres, J.A. Queiroz, Biomed. Chromatogr. 21 (2007) 993.
[26] N.L. Krajnc, F. Smrekar, A. Strancar, A. Podgornik, J. Chromatogr. A (2011), doi:10.1016/j.chroma.2010.12.058.